

# Reliability Analysis of Failed Slopes, a Back Analysis View of the Sensitivity to Input Parameters

J.D. ST GEORGE

B.Sc., M.Sc., A.R.S.M., M.I.M.M.

Senior Lecturer, Department of Mining Engineering, University of Auckland

## 1. INTRODUCTION

In probabilistic analyses the uncertainties associated with the problem are included within the framework of the analysis, therefore the risks associated with the consequences of various strategies can be evaluated in terms of selected design criteria. Extensive literature on the probability of failure related to slope analysis has been published, mostly confined to theoretical development with few trial or hypothetical slopes investigated. Those studies which have been reported require a great deal of statistical data for a full analysis and generally represent slopes which have a very low failure probability. In this work slope failures from surface coal mines are back analysed using a reliability approach.

A probabilistic model has been developed which is capable of incorporating variations in shear strength, modelling errors and watertable. The variability of the shear strength parameters were considered to be a combination of spatially correlated variations and independent components. A further refinement to include 3-D effects from end resistance and variance reduction along the failure length, provided a means of estimating the probability of failure for different lengths and volumes. These could then be compared to actual failure volumes. This paper presents a background to the techniques and the basis for the model, it then reviews the case studies and investigates the sensitivity to input variables with respect to the failure analysis.

## 2. UNCERTAINTIES IN SLOPE ANALYSIS

There are many variables that enter into slope analyses and with a probabilistic approach, the uncertainties associated with these variables need to be quantified and included in the analysis. Subjective uncertainties, from a lack of knowledge or information, necessitate the use of deductive reasoning and therefore will never be totally eliminated. They are usually allowed for by conservative, flexible design procedures and the observational approach advocated in many engineering projects. It would be unreasonable to expect the techniques of risk analysis and statistics to resolve problems which cannot be formally answered, and as such are not introduced directly into the analysis. Objective uncertainties which can be recognized and to some extent be quantified, are related to measured statistical or probabilistic information. The major uncertainties in a slope stability analysis arise from the natural heterogeneity in the shear strength ( $c$  and  $\phi$ ) of geological materials, structural controls on failure, water conditions and model assumptions. These

are further compounded by sampling and testing techniques. Minor variations from inaccurate measurements of slope geometries and variability in material properties (i.e. density and permeability) are not treated separately as they do not influence the stability analysis to the same extent. The main contribution to these uncertainties are discussed in the following sections.

### 2.1. Variability in Shear Strength

Within so-called homogeneous geological units the shear strength is known to vary widely from point to point. No amount of testing can fully characterise the nature of this heterogeneity, and therefore some probabilistic uncertainty will always remain. The variability in shear strength, in most cases, is dependent on location and as such is spatially correlated. This regionalised behaviour implies that points in close proximity are strongly correlated as would be reasonable to expect from the natural processes involved in their formation or in the method of placement for man-made slopes. The correlation will diminish as the distance between points becomes larger, until the covariance between points is zero. This spatial dependence has other implications that are introduced later in the analysis. The sampling and test results present a different problem in that they contain inferential uncertainties. These are quantifiable and can be reduced to an arbitrary level by increasing the sample size. However they will also introduce bias errors for the following reasons.

During the recovery and preparation process, it is unavoidable to prevent some mechanical disturbance to the sample. Stress conditions on the boundary will change as a result of removal from the in situ stress field and little is known about the induced stresses caused by sampling. The results from laboratory shear or triaxial tests are used to predict the behaviour of a slip surface many orders of magnitude larger. The influence of macro effects or scaling remain essentially unsampled. The testing techniques present inherent differences between actual conditions and the simulated laboratory test. These problems may be partially avoided by testing large scale samples in situ, however it is difficult to exercise full control over the test environment in the field and this contributes to the overall uncertainty.

### 2.2. Water Conditions within Slope

Most uncertainties concerned with determining the watertable or pore pressures within a slope are from a lack of information and are therefore subjective.

The prediction of the water pressures within the slope from very limited information usually involves gross, order or magnitude assumptions about infiltration rates, position of aquifers, aquicludes, flow, permeabilities, and presence of perched aquifers or artesian conditions. Water pressures estimated from measuring sites within a slope will have a statistical uncertainty from the interpolation between measuring stations. Meteorological data introduces more variables into the problem.

### 2.3. Structural Controls on Failure

When the geometry of a slope failure is governed by structural features (discontinuities), for example wedge failures in rock slopes, an uncertainty is introduced at the level of the mechanism. This is because there will be variability in the dips, dip directions, spacing and length of discontinuities controlling the failure as well as those errors associated with the measurement of these parameters. With enough information there are techniques which allow for the mechanisms to be modelled probabilistically quite successfully. Unfortunately the field data is seldom available in the areas of interest and extrapolation of structural data is problematic and in itself stochastic.

### 2.4. Model uncertainty

Further uncertainty arises from the simplifying assumptions made in the analytical model. Therefore, even if all input parameters to a particular model were known exactly, there would be an uncertainty associated with the output. From the very nature of the simplifying assumptions in the analytical models, part of these uncertainties are biased. In the absence of any significant data the design engineer may have to make a subjective estimate for the model uncertainty.

It is apparent from the above comments that in risk assessment of a slope failure, it is only possible to model those uncertainties that are measurable, unless some 'judgement factor' is included. The risks are expressed in the form of a probability or reliability, which can then be applied to design decisions. The objective uncertainties relate to two fundamental areas in slope analysis, firstly the failure mechanism and secondly to the analysis - input parameters and calculation process. The true variation of input parameters can never be determined completely since any sampling will only be partial and the unknown inaccuracies present in testing techniques can not be quantified. This lack of information particularly in respect to the shear strength and watertable will require the use of deductive reasoning to resolve. In this paper no attempt has been made to examine the effects of structural controls on the failure mechanisms since no quantitative data was available for the case studies. The uncertainties associated with the variability in shear strength, water conditions and modelling error have been investigated within a probabilistic slope analysis.

## 3. MODEL DEVELOPMENT

The first stage of a probability based slope analysis is to quantify the possibility of failure, the second being to rationalise the consequence of failure. The probability of failure  $P(\text{Slope failure})$

is denoted by  $P_f$ . The procedures for analysing slope failures are the same as in ordinary deterministic methods - limiting equilibrium, stress-deformation or plasticity models. Because of the generally sparse information available, the simplicity and wide acceptance in deterministic analyses of limiting equilibrium or slice techniques, these are favoured for probabilistic analyses. Using the factor of safety  $F$  defined as the ratio of resisting ( $R$ ) to mobilising ( $S$ ) forces or moments, the probability of failure is defined as  $P(F < 1.0)$  or  $P(R < S)$ .

Initially a distinction is required between the failure probability of one specific failure surface and the slope as a whole. The  $P_f$  may refer to a specific location along the slope, for one cross section and the analysis is confined to two dimensional plane strain failures in that section. Alternatively a complete length of slope or a geologically homogeneous unit is treated as one entity, the  $P_f$  applying to the whole section. In a homogeneous material free from structural controls, there are an infinite number of kinematically possible failure surfaces for any given cross section. These will represent the family of curves, circular, log spiral or non-linear, each contributing to the overall  $P_f$ . Cornell (1971) argued that these potential failure surfaces represented components of a series system and since many of these surfaces would be in close proximity, their probabilities would be highly correlated. The overall system reliability would therefore be close to the surface with the highest  $P_f$ . Alonso (1976) has shown by a case study of circular failure in a homogeneous material that the surface with the highest  $P_f$  corresponds to that with the minimum factor of safety  $F$ . More recently Sharp (1982) and Chowdhury and Zhang (1988) have demonstrated that this is only true for certain statistical parameters.

The probability of sliding represents in a single figure the frequency of conditions that cause a particular slope geometry to fail, as a proportion of all possible conditions. In order to calculate this probability either the full distribution of the random input variables or their moments are required. These are then combined in an appropriate probability model, taking account of modelling errors, to produce the distribution of failure conditions, or its moments.

Second moment analysis has been favoured in place of full distribution methods, because no assumptions are required regarding the distributions of the input variables. Two techniques are commonly referred to in the literature: these are point estimates and the first-order second moment method (FOSM). In the latter method it is possible to model the spatial variability and the covariance between the shear strength parameters, as demonstrated by Alonso (1976) and therefore this method was preferred. To analyse failure geometries of any shape, the simplified Janbu method, Janbu(1973) was formulated in a FOSM approach. Approximations of the mean and variance of the factor of safety are determined from first-order expansion terms of a Taylor series. Full details of the equations are given in St George (1991). In all second moment methods it is necessary to assume some distributional form of the factor of safety or safety margin to calculate a probability of failure. It is convenient to assume a normal distribution and calculate probabilities from standard tables. For comparative purposes the reliability index  $\beta$  is a useful parameter, defined from the mean and standard deviation of the factor of safety by

$$\beta = \frac{F_s - 1}{\sigma_f} \quad \dots(1)$$

To incorporate the spatial variability of the shear strength it is necessary to calculate the covariance between points within the slip surface. This requires some correlation function to be defined. An approach from the theory of regionalised variables was developed to estimate this covariance. Firstly the spatial behaviour must be characterised. This information is contained in the form of a variogram which is the compliment to the covariance function. Normally the process involves fitting parameters for a number of general models to the field data and then selecting the most appropriate model. Since it was the intention here to investigate the influence of spatial variability a general model was selected and the parameters were varied. The exponential variogram model was chosen because it has a convenient mathematical form and is a monotonically increasing function with a sill (C). This sill represents the independent variance and occurs when point spacing exceeds the range of influence (a). A nugget effect  $C_0$  is included which accounts for the non-spatial contribution to the overall variance. The general form of the exponential function variogram is

$$\gamma(h) = C_0 + C(1 - e^{-h/a}) \quad \dots(2)$$

If either  $a = 0$  or  $C = 0$ , the model reduces to the spatially uncorrelated component  $C_0$ .

A quasi 3-D approach developed by Vanmarcke (1977b) incorporates the spatial variability along the slope together with the resistance at the lateral margins of the potential failure and produces a 3-D probability of failure. This approach has a lot of appeal since it only requires the mean and variance from the 2-D plane strain solutions and variance reduction function, end resistance and failure length (b) to find the 3-D  $P_{fb}$ . The variance reduction function  $\Gamma^2$  takes into account the spatial variability along the slope. To make this consistent with the spatial model in 2-D, a function was chosen which modelled the same characteristic behaviour as the exponential variogram. Vanmarcke (1977a) has shown that the reduction function  $\Gamma(b)$  defined as

$$\Gamma(b) = \begin{cases} 1 & b \leq \delta \\ \left(\frac{\delta}{b}\right)^{\frac{1}{2}} & b > \delta \end{cases} \quad \dots(3)$$

provides a close approximation to the exponential correlation function if  $\delta$  the scale of fluctuation is equal to twice the range.

In order to calculate the resistance at the ends of the failure, assumptions regarding the strength and stress conditions are required. It is inevitable that these will only be approximate, and depend on localized conditions. Initially the stress distribution on the lateral margins is assumed to result from active earth pressures and the resisting forces at each end may be calculated using the shear strength. A lateral release factor ( $\alpha$ ) is proposed which takes into account structural and geometrical effects on release. The total end resistance is determined from  $R_e = \alpha_1 R_{e1} + \alpha_2 R_{e2}$ , where the subscripts refers to each end of the failure. Spatial variability of the lateral margins was neglected as its contribution to the overall variance would be small.

The contribution to the total resistance from the strength of the lateral margins is usually ignored in conventional 2-D analyses because the resulting F is conservative. In the 3-D probabilistic model, as the failure width (b) increases the contribution

from the lateral margins as a proportion of the total resistance, will reduce. At the limit for long slope widths the 3-D safety factor  $F_b$  will be equivalent to the plane strain 2-D F. Also as the failure width (b) increases, the variance of the 3-D factor of safety is attenuating from the unit width variation. Therefore provided  $F > 1.0$ , short failure widths will have low 3-D probabilities of failure  $P_{fb}$  due to a high  $F_b$  from the end resistance and the  $P_{fb}$  for long failures will also be small due to the low variance in  $F_b$ . This variance reduction concept is applicable whether or not the variables are spatially correlated. Vanmarcke (1977b) derived a critical width  $b_c$  for a cylindrical failure area which minimises the reliability index and consequently maximises  $P_{fb}$ . Using the reduction function in equation (3), the critical width  $b_c$  is approximated by

$$b_c = \frac{F}{F-1} d_0 \quad \dots(4)$$

Where  $d_0$  is a function of end section geometry and the failure surface and F is the plane strain factor of safety. For these assumptions  $b_c$  is independent of the rate of variance reduction.

Both the 2-D and 3-D probabilistic models have been programmed in Fortran 77. Besides the slope and failure surface geometries the input parameters are as follows:

- Shear strength: Mean and standard deviation of c and  $\phi$  for each material and lateral margins.
- Spatial: Sill C, nugget effect  $C_0$  and range of influence a
- Failure width b
- Lateral release factor  $\alpha$
- Model error
- Coefficient of watertable variation

The results from each analysis produced a 2-D F and a 3-D  $F_b$  with their respective reliability indices and probabilities of failure, making the assumption of a normal distribution. The critical failure width defined in equation (4) was also calculated, approximating  $d_0$  from the ratio of section area to length of failure arc. The variance reduction parameter, the scale of fluctuation, was set at  $2a$ , although deviations from this can be made during program execution.

#### 4. CASE STUDIES

The majority of cases for this work were taken from an extensive study of failures in UK opencast mines, conducted by the Department of Mining Engineering, University of Nottingham. A review of this work is presented by Stead (1984). The failures recorded by Chandler (1974) were included as a control to test the algorithms but as no failure lengths were recorded, these cases were not included in the 3-D analyses. All the case studies have been recorded on a database system and are identified by a group code and number. The groupings are made according to the material on the failure surface and are listed in Table I. Individual failures are referenced by the group code and number, e.g. LIAS\_301 and SEAT\_79.

Each group is representative of a particular geologic material and should display reasonably consistent properties. The material properties from each group were taken from published test results. The standard deviation for these parameters was obtained by comparing the range of the data with a coefficient of variation of 40% for cohesion and 20% for  $\phi$ , the lower value was used in the analysis.

Table I  
 Case Studies Under Material Grouping

Group	Code	Number	Description
Lias Clay	LIAS	8	Brecciated and unbrecciated clay.
Loosewall	LWCC	14	Backfill materials - circular failure mechanisms only.
Loosewall	LWBP	11	Biplanar failures with basal materials having weaker strength than backfill.
Seatearth	SEAT	17	Majority of failure plane within seatearth material.
Clayband	CLBD	13	Failure plane confined to bedding features with high clay content.

5. ANALYSIS

The sensitivity of the input variables was initially studied in 2-D taking the observed failure geometries, thereby removing this uncertainty from the analyses. The parameters which were independent of the variability in shear strength, i.e. model error and watertable, were investigated first.

**Model error:** This term is added to the overall variance and will therefore increase the  $P_f$  ( $P_f < 50\%$ ). Figure 1 is a plot of  $P_f$  versus model error for two Lias Clay failures showing the expected increase in  $P_f$  as the model error becomes more significant. For the remainder of this work the error was kept constant at 5%. This is consistent with the expected accuracy of limit equilibrium methods.

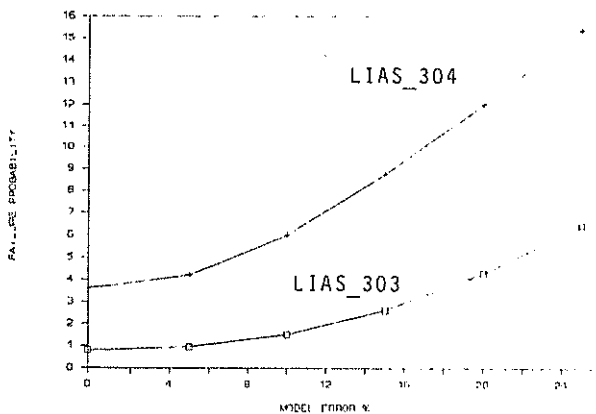


Figure 1 Sensitivity to model error

**Watertable:** It has been assumed that on the scale of the cross sections, the watertable or pore pressures are completely correlated. The variations are therefore just additive on the overall variance and have a similar effect on the  $P_f$  as model error. The upper and lower estimates for the phreatic surface were made on the basis that they covered all probable conditions consistent with slope observations and any measurements. A dry or fully drained slope would represent the lower limit. The upper limit is less reliable to estimate although a fully saturated slope would represent a maximum watertable in the absence of artesian conditions. The same Lias Clay cases show, in Figure 2, the effect of changing the coefficient of variation of watertable on  $P_f$ .

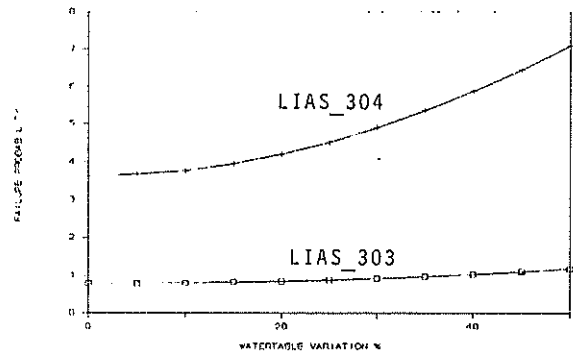


Figure 2 Sensitivity to watertable variations

The variability in the shear strength is related to the individual variance of  $c$  and  $\phi$ , their spatial correlation and the correlation between them. Intuitively the presence of spatial correlation will cause a reduction in the overall variance for the shear strength. In order to study this effect, different ranges or autocorrelation distances (5-200m) were compared to the completely uncorrelated  $P_f$ . It was found that the size of failure influenced the behaviour of  $P_f$  with respect to the range of influence. For the large failures the  $P_f$  decreased initially on increasing the range until some minimum point was achieved. Then gradually increased asymptotically to the uncorrelated value. For the small scale failures this effect was probably masked ( $a < 5$ ) as they only showed an increase towards the uncorrelated values. The  $P_f$  is plotted against the range of influence (a) in Figure 3, for the large (LWCC\_104) and small (LWCC\_129) failures.

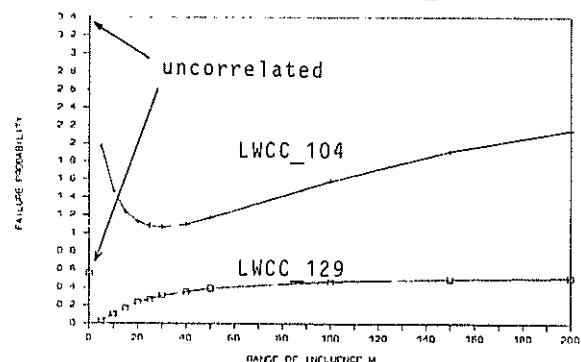


Figure 3 Effect of range of influence on  $P_f$

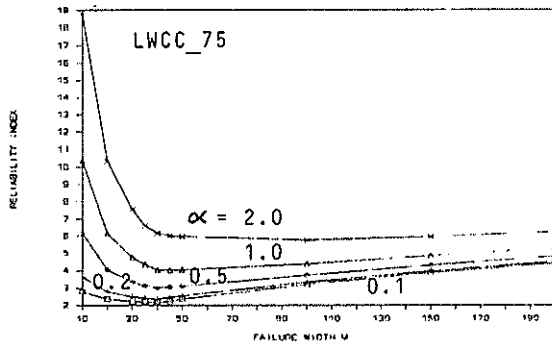


Figure 4 Effect of lateral release on  $\beta$

Correlation between the shear strength parameters  $c$  and  $\phi$  was investigated by varying the correlation coefficient from -1 to +1. The changes in  $P_r$  were very small and, as expected, positive correlation contributed to an increase, negative correlation a decrease in  $P_r$ .

Extending the analysis to 3-D introduces the lateral release factor ( $\alpha$ ), variance reduction function and the scale of fluctuation. The resistance on the lateral margins also requires a shear strength value. In case studies where failure through the lateral margins occurs in essentially intact material, a strength representative of that material was used e.g. loosewall slopes. For rock slopes where intact strength is high, release occurs along discontinuities and a uniform strength of  $\phi=30^\circ$   $c=0kPa$  was assumed. Then  $\alpha$  measures the relative strength of release to this standard value. The lateral release factor directly affects the 3-D factor of safety  $P_b$  and in the limit as failure width  $b \rightarrow \infty$ ,  $P_b$  converges to  $F$ .

The form of the reduction function and scale of fluctuation have been chosen to be consistent with the 2-D spatial behaviour and therefore the 3-D model will be essentially controlled by the range of influence ( $a$ ). By holding the range constant, the effect of variations in end resistance, on  $P_b$ , can be observed. This is achieved by varying the lateral release factor with both ends of the failure having the same  $\alpha$ . Figure 4 shows the reliability index ( $\beta$ ) plotted against failure width ( $b$ ) at different lateral release factors for case study LWCC\_75. As can be seen the critical failure width  $b_c$  defining a minimum  $\beta$  (maximum  $P_b$ ) is dependent on the lateral release factor. The critical failure widths becoming shorter with reducing end resistance, as would be expected. It clearly shows the influence  $\alpha$  has on the reliability index. At the observed failure width for the slope (100m),  $\beta$  changes from 3.2 ( $\alpha=0.1$ ) to 5.7 ( $\alpha=2.0$ ). This effect will be amplified for rock slopes where strength differences between intact rock and discontinuities are high. Other factors such as slope curvature helping release also appear to be important in these cases.

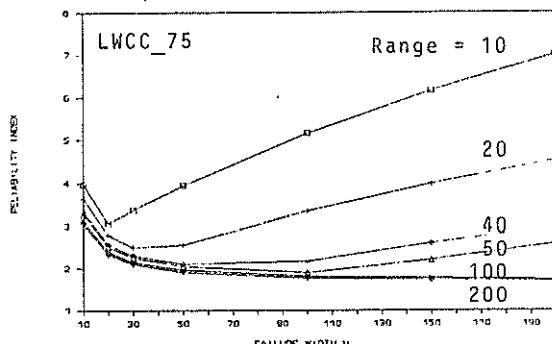


Figure 5 Effect of range of influence on  $\beta$

By holding the lateral release factor constant ( $\alpha=0.2$ ), the effect of spatial correlation on the reliability index is investigated. Figure 5 shows a plot of failure width versus reliability index for different ranges of influence ( $a$ ) for the same case study. It clearly demonstrates that the minimum  $\beta$  is also dependent on the range. The critical failure width  $b_c$  calculated using equation (4) was compared to the actual failure widths and have been plotted as a ratio in Figure 6. Three cases are not included due to excessive predicted failure lengths; the largest being 2741m for an actual failure length of 150m, and those cases with  $F < 1$ ,  $b_c$  is undefined. A further indication of failure length was obtained from examining the cross section length  $L_{xs}$  of the failures. It was noted the majority of actual failures were within  $1 < L_{xs} < 3$ . Failure lengths longer than  $3L_{xs}$  were attributed to being essentially multiple events. There was only one failure noticeably shorter than  $L_{xs}$  and this was caused by over steepening at the toe, along a portion of the slope.

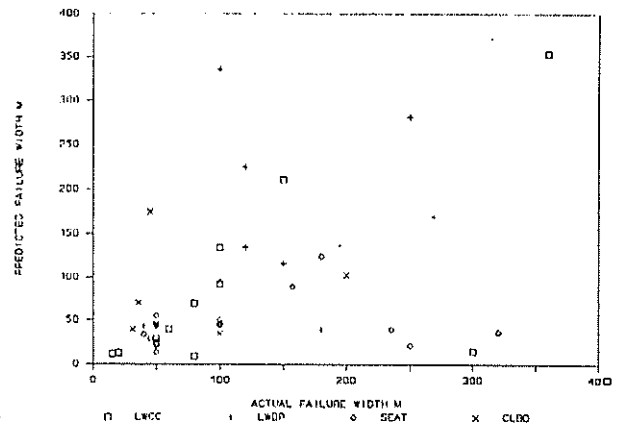


Figure 6 Actual vs predicted failure widths

In order to use the 3-D  $P_b$  in a predictive analysis the slopes were re-examined without regard to the actual failure plane. The loosewall cases were all analysed in this way and compared to the actual failures. Two failure modes were investigated circular and biplanar. The critical circular slip surfaces with the minimum 2-D  $F$  were located by standard search routines and this was then compared to the lowest  $F$  from the biplanar analysis. The dip of the pavement was assumed known, with a strength of  $c=0kPa$  and  $\phi=16^\circ$ . The lowest overall  $F$  defined the failure geometry; then the critical failure width  $b_c$  and  $L_{xs}$  were calculated for this cross section if  $L_{xs} < b_c < 3L_{xs}$ ;  $b_c$  was taken as the failure length, otherwise  $L_{xs}$  was used. The  $P_b$  was calculated for this failure width. The spatial variability was modelled with a range of 100m. The lateral release factor, in all cases, was set to 1, since side release would occur through spoil material. The results are presented together with the actual failure widths and volumes in Table II. Also included are time to failure and water rating for the slopes. The cases are listed in ascending order of probability and it is evident the very low  $P_b$  values have a delayed failure and/or water has been an important component. The predicted failure widths and volumes deviated considerably from the observed which is perhaps indicative of the lowest 2-D  $F$  not producing the maximum 3-D  $P_b$ . All those failures with a  $P_b > 5\%$  water appears to be a significant factor, except for LWBP\_83 where no information was available. The two cases with  $P_b$  much greater than 50% (LWCC\_169 and LWBP\_183) were examples of extremes. LWCC\_169 had a slope angle of  $60^\circ$  to a height of 33m while LWBP\_183 was cut at  $40^\circ$  to a height of 80m on an  $8^\circ$  dipping pavement. Even with optimistic strength parameters both these cases

TABLE 2

Failure Probabilities for Loosewall Case Studies

Code	Probability of Failure $P_{fb}$	Predicted		Actual		Time Factor	Water Factor
		Volume $\times 10^3 m^3$	Width m	Volume $\times 10^3 m^3$	Width m		
LWCC_79	$6.4 \times 10^{-5}$	67	87	6	60	4	3
LWBP_17	$3.1 \times 10^{-3}$	38	80	176	180	2	4
LWBP_44	$2.5 \times 10^{-2}$	1009	244	500	250	4	3
LWCC_192	$3.5 \times 10^{-2}$	6	37	13	50	4	1
LWBP_144	$5.1 \times 10^{-2}$	36	83	50	150	3	3
LWCC_129	$6.6 \times 10^{-2}$	1	17	0	15	2	0
LWCC_172	$8.9 \times 10^{-2}$	3	30	5	80	2	2
LWCC_219	0.16	30	64	28	80	3	3
LWCC_69	0.18	4	32	30	300	2	1
LWCC_152	0.33	1	22	1	50	2	0
LWCC_239	0.72	1	19	1	20	3	3
LWBP_217	0.72	303	129	368	120	2	1
LWBP_201	0.77	67	108	87	120	3	4
LWCC_75	1.12	36	91	51	100	1	1
LWCC_199	3.38	28	78	36	100	2	2
LWBP_150	4.77	11	41	5	100	4	0
LWBP_155	8.24	9	39	21	90	2	4
LWBP_83	20.90	2	39	2	40	2	0
LWBP_177	31.80	210	148	728	150	1	3
LWCC_104	50.20	247	145	135	360	4	3
LWCC_169	82.30	8	42	8	25	3	3
LWBP_183	99.80	188	125	466	200	3	3

Time Factor		Water Factor	
0	No details	0	No details
1	< 1 week	1	Dry/fully drained
2	1 week - 1 month	2	Slight seepage/rainfall
3	1 - 3 months	3	Heavy seepage/rainfall
4	3 - 6 months	4	Artesian conditions

have 2-D F below 1 for dry conditions. The other case with  $P_{fb} > 50\%$ , LWCC\_104 had a submerged toe due to the formation of a sump, this would explain the long time to failure since the dry  $P_{fb}$  for same geometry was  $5.1 \times 10^{-3}$ . For case studies with  $P_{fb}$  above  $5 \times 10^{-2}$  and below 5%, there is reasonable concordance between measured and predicted volumes and failure widths. One notable exception is for LWCC\_69 where the observed failure width is a factor of 10 greater than predicted.

## 6. CONCLUSIONS

From the 2-D analysis it was noted how the  $P_f$  was sensitive to changes in model error and watertable variations. The effect of spatial and parameter correlation had a lesser influence on  $P_f$ , however the behaviour of  $P_f$ , with respect to spatial variability, was found to be dependent on the scale of failure. The most significant influence on the 3-D  $P_{fb}$  was the resistance of the lateral margins and clearly this represents an area where more research could be carried out. The form of the variance reduction function altered  $P_{fb}$  and also affected the so-called critical failure width where the minimum  $\beta$  is defined. The retrospective analysis of the loosewall failures produced mixed results. Those cases with very low  $P_{fb}$  did not measure up in terms of failure geometries, widths and volumes with the observed failures. However there was good agreement between volume and failure width for most of the other cases and this might provide a means of estimating potential failure volumes. As the 3-D  $P_{fb}$  is sensitive to lateral release, the presence of weak planes or slope curvature will greatly reduce the probability of failure, particularly for rock slopes. The critical failure width would become less important since the potential failures would be positional, related to release features on the slope.

## 7. REFERENCES

- Alonso E. (1976) Risk Analysis of Slopes and its Application to Slopes in Canadian Sensitive Clays, Geotechnique, 26, No 3, 453-472.
- Chandler, R.J. (1974) Lias Clay: The long-term stability of cutting slopes, Geotechnique, 24, No 1, 21-38.
- Chowdhury R.N. and Zhang S. (1988) Prediction of Critical Slip Surfaces, 5th Australia-New Zealand Conf on Geomechanics, Sydney, 451-455.
- Cornell G.A. (1971) First Order Uncertainty Analysis of Soils Deformation and Stability, Proc 1st ICASP-SSE, Hong Kong.
- Janbu N. (1973) Soil Stability Computations, Embankment Dam Engineering, Casagrande Volume, Wiley, New York, 47-87.
- Sharp K.D. (1982) Development of a Model for Probabilistic Slope Stability Analysis and Application to a Tailings Dam, PhD Thesis, University of Utah.
- Stead D. (1984) An Evaluation of the Factors Governing the Stability of Surface Coal Mine Slopes. PhD Nottingham University.
- St George J.D. (1991) Probabilistic Methods Applied to Slope Stability Analysis, unpublished PhD thesis, Auckland University.
- Vanmarcke E.H. (1977a) Probabilistic Modelling of Soil Profiles, J of Geotech Engng Div ASCE, 103, GT11, 1237-1246.
- Vanmarcke E.H. (1977b) Reliability of Earth Slopes, J of Geotech Engng Div ASCE, 103, GT11, 1247-1266.